Journal of Thermal Analysis and Calorimetry
https://doi.org/10.1007/s10973-020-09628-5

# Thermogravimetric and kinetic study of new bis(iminophosphorane) ethane solvates

**Manuela E. Crisan[1] · Gabriela Vlase[2] · Titus Vlase[2] · Lilia Croitor[1,3] · Gheorghe Ilia[1,2] · Paulina N. Bourosh[3] · Victor Ch. Kravtsov[3] · Mihaela F. Petric[1]**

Received: 4 October 2019 / Accepted: 23 March 2020


**Abstract**
Thermal and crystallographic characterization of one solvent-free bis(iminophosphorane)ethane (BIPE) form and three solvates with acetonitrile (ACN), dimethyl sulfoxide (DMSO) and toluene is presented. Thermal behaviors of new compounds indicate that the solvent is removed differently from the BIPE structure, accordingly with the stoichiometric solvent molecule amount incorporated. Thus, the solvent-free BIPE reveals high thermal stability up to 315 °C, while BIPE solvates have a similar pattern behavior with low stability about 130 °C. The kinetic parameters of the thermal decomposition process were determined by three different methods Flynn–Wall–Ozawa, Kissinger–Akahira–Sunose and nonparametric kinetic. Crystallographic data revealed that the solvent plays the role of space filler without strong interactions with host molecules. Guest-free BIPE, $BIPE_{0.5ACN}$ and $BIPE_{0.35DMSO}$ crystallized in monoclinic *C*2/*c* (№15) space group, while $BIPE_{TOLUENE}$ in a triclinic *P* - 1 (№2) one. Crystallographic and thermogravimetric data show a good correlation between molecular structures and activation energies.

**Keywords** Bis(iminophosphorane)ethane · Solvates · Single crystal X-ray diffraction · Thermal stability · Non-isothermal kinetics

## Introduction

Numerous studies suggest an increasing number of new solvates demonstrating their significant role in organic synthesis, crystal engineering and pharmaceutical drug development [1–3]. Depending on the stoichiometric/non-stoichiometric amounts, the solvent molecules can have different structural functions in organic compounds, for example as participants in strong intermolecular interactions with the host molecules, leading usually to stoichiometric solvates [4, 5] and as space fillers between solute molecules, with no strong interactions between the solvent and solute molecules [6]. The last ones may be often non-stoichiometric solvates with the partial occupancy of their solvent molecules positions in the crystal where solvent molecules decrease the total void spaces and improve the packing [7].

In this context, it is very interesting to study the cases of different solvent molecules incorporation in the same host structure which give the isostructural solvates. They allow establishing the identical packing motifs of the host molecule with common sites of solvent positions [8]. The relation between molecular shapes of the guest molecule, solvent-host interactions, and formation of isostructural solvates were ascertained [9, 10]. However, a number of publications which highlight this phenomenon is very limited and it requires more attention. Over the last years, classification of solvents which form solvates has changed and the tendency to use toluene instead of benzene increases due to its lower toxicity, besides other top popular solvents such as acetonitrile (ACN), dimethylformamide (DMF), dimethyl sulfoxide (DMSO) and dioxane [11, 12].

✉ Titus Vlase
titus.vlase@e-uvt.ro

✉ Mihaela F. Petric
mihaelapetric@yahoo.com

[1] "Coriolan Dragulescu" Institute of Chemistry, 24 Mihai Viteazul Boulevard, 300223 Timisoara, Romania

[2] Research Center: Thermal Analysis in Environmental Problems, West University of Timisoara, Pestalozzi Street 16, 300115 Timisoara, Romania

[3] Institute of Applied Physics, 5 Academiei Street, 2028 Chişinău, Republic of Moldova

Published online: 04 April 2020

Thermogravimetry and single-crystal X-ray diffraction are valuable analyses for studying and understanding the solvates formation and their stability. Herein, we present the crystal structures and thermal kinetic behavior of new bis(iminophosphorane)ethanes (BIPE), one solvent-free form and three solvates with ACN, DMSO and toluene (Scheme 1). Despite the versatility of BIPE to act as valuable building blocks in organic, organometallic and coordination synthesis of biologically active compounds [13–15], only two organic crystal structures with ethane spacer between iminophosphorane fragments are currently known [16–18]. Nature and inclusion mode of different solvent molecules within the framework formed by the host were investigated comparatively. Combination of thermogravimetric analysis, differential thermal analysis and single-crystal X-ray diffraction were used.

## Experimental

### Materials and physical measurements

All used reagents (diphenylphosphoryl azide and 1,2-bis(diphenylphosphino)ethane) and solvents (DMF, ACN, DMSO and toluene) were acquired from commercial sources in analytical purity and were used without further purification.

Thermal behavior was determined using a Diamond Thermobalance TG/DTA PerkinElmer in a dynamic air atmosphere (synthetic air 5.0 Linde Gas with flow 100 mL $min^{-1}$). The experiments were carried out from 25 °C up to 500 °C, at heating rates $\beta = 7$, 10, 12, 15 and 20 °C $min^{-1}$, and masses around 8 mg of samples were weighted in open aluminum crucibles.

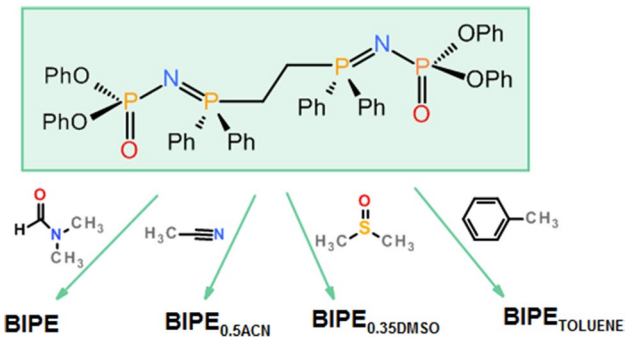


**Scheme 1** The preparation of BIPE compounds in different solvents

### Synthesis of compounds BIPE, $BIPE_{0.5ACN}$ and $BIPE_{0.35DMSO}$

Bisiminophosphoranes BIPE, $BIPE_{0.5ACN}$ and $BIPE_{0.35DMSO}$ were synthesized according to Staudinger method [16, 19, 20] in DMF (BIPE), ACN ($BIPE_{0.5ACN}$) and DMSO ($BIPE_{0.35DMSO}$) at room temperature. Colorless crystals were precipitated after a few days and were purified by recrystallization in the appropriate solvents.

### X-ray crystallography

Diffraction measurements for compounds BIPE, $BIPE_{0.5ACN}$ and $BIPE_{0.35DMSO}$ were carried out at room temperature on an Xcalibur E diffractometer equipped with CCD area detector and a graphite monochromator utilizing MoK$\alpha$ radiation. Final unit cell dimensions were obtained and refined on an entire data set. All calculations to solve the structures and to refine the proposed models were carried out with the SHELXL2014 program package [21]. All non-hydrogen atoms were refined anisotropically. Hydrogen atoms attached to carbon and nitrogen atoms were positioned geometrically and treated as riding atoms. In $BIPE_{0.35DMSO}$ crystallization, DMSO molecule is disordered over two positions (71/29% occupation). The disordered DMSO molecule has been well treated by restraining it to have the SAME geometric parameters as the well-determined ordered DMSO molecule and was refined isotropically. The X-ray data and the details of the refinement for both compounds are summarized in Table 1. Figure 1 was produced using the Mercury program [22]. The solvent accessible voids (SAVs) were calculated using PLATON [23]. Crystallographic data of the new compounds reported herein were deposited with the Cambridge Crystallographic Data Centre and allocated the deposition numbers CCDC 1956713–1956715.

## Results and discussions

Bis(iminophosphorane)ethanes BIPE, $BIPE_{0.5ACN}$ and $BIPE_{0.35DMSO}$ crystallize in the centrosymmetric monoclinic space group $C2/c$ (№15) and are isostructural (Table 1), in contrast to toluene solvate ($BIPE_{TOLUENE}$) which crystallizes in a triclinic $P-1$ (№2) space group [16]. All structures adopt almost the same packing arrangements, with solvent molecules incorporated in the crystal lattice via weak hydrogen-bond interactions. In the $BIPE_{0.5ACN}$ and $BIPE_{0.35DMSO}$ compounds, solvent molecules are involved in the C–H···N(O) intermolecular interactions with host molecule, C31···N1A = 3.658 Å, C16···O1S = 3.353 Å and C37···O1S = 3.566 Å (Fig. 1a). In $BIPE_{TOLUENE}$ solvent,

**Table 1** Crystallographic data and structure refinement details for compounds BIPE, $BIPE_{0.5ACN}$ and $BIPE_{0.35DMSO}$

| | BIPE | $BIPE_{0.5ACN}$ | $BIPE_{0.35DMSO}$ |
|---|---|---|---|
| Empirical formula | $C_{50}H_{46}N_2O_6P_4$ | $C_{51}H_{44}N_{2.50}O_6P_4$ | $C_{50.70}H_{46.10}N_2O_{6.35}P_4S_{0.35}$ |
| Formula mass | 894.77 | 911.76 | 920.09 |
| Temperature/K | 293(2) | 293(2) | 293(2) |
| Wavelength/Å | 0.71073 | 0.71073 | 0.71073 |
| Crystal system | Monoclinic | Monoclinic | Monoclinic |
| Space group | *C*2/*c* | *C*2/*c* | *C*2/*c* |
| *Z* | 8 | 8 | 8 |
| *a*/Å | 41.006(4) | 41.180(3) | 41.2529(15) |
| *b*/Å | 11.1370(8) | 11.2006(5) | 11.1604(3) |
| *c*/Å | 20.9175(12) | 21.0745(10) | 21.1627(7) |
| *β*/° | 110.110(6) | 111.007(5) | 110.680(3) |
| *V*/Å$^3$ | 8970.3(12) | 9074.4(9) | 9115.5(5) |
| $D_c$/g cm$^{-3}$ | 1.325 | 1.335 | 1.341 |
| μ/mm$^{-1}$ | 0.221 | 0.220 | 0.236 |
| *F*(000) | 3744 | 3804 | 3846 |
| Crystal size/mm$^3$ | 0.60 × 0.25 × 0.20 | 0.30 × 0.20 × 0.17 | 0.38 × 0.36 × 0.20 |
| Reflections collected/unique | 14,256/7843 ($R$(int) = 0.0366) | 15,002/7960 ($R$(int) = 0.0499) | 27,869/8079 ($R$(int) = 0.0491) |
| Reflections with [$I > 2\sigma(I)$] | 4690 | 4107 | 4977 |
| Data/restraints/parameters | 7843/0/559 | 7960/0/565 | 8079/6/615 |
| GOF on $F^2$ | 1.001 | 0.979 | 1.007 |
| $R_1$, w$R_2$ [$I > 2\sigma(I)$] | 0.0566, 0.1161 | 0.0678, 0.1276 | 0.0534, 0.1091 |
| $R_1$, w$R_2$ (all data) | 0.1106, 0.1355 | 0.1460, 0.1539 | 0.0983, 0.1276 |

toluene molecule are accumulated in the crystal lattice via C−H···π interactions, with carbon atom…phenyl ring centroid distance equal with 3.189 Å (Fig. 1b). The structure of guest-free iminophosphorane BIPE contains negligible 322.4 Å$^3$ solvent accessible voids (SAVs), which corresponds to about 3.6% of unit cell volume [23]. No SAVs were found in solvate structures $BIPE_{0.5ACN}$ and $BIPE_{0.35DMSO}$. The calculated volumes occupied by these solvent molecules in discussed compounds are represented in Table 2.

## Thermal analysis

Thermogravimetry (TG) and derived thermogravimetry (DTG) were performed in the air atmosphere to analyze the thermal behavior of the studied sample. The result is shown in Fig. 2 and proved that the guest-free BIPE is stable up to 315 °C. Thermoanalytical curves obtained in the atmosphere of synthetic air at a speed of 10 °C min$^{-1}$ show one decomposition step for BIPE. On the Heat Flow (HF) curve, an endothermic process can be observed, which is attributed to the melting of the compound with a maximum at 138 °C. The decomposition process highlighted in the range 315.6–430.9 °C occurs with a loss of 66.54% of the sample mass. Analyzing the DTG and HF curves, it is observed that within this interval at least two decomposition processes take place, both exotherms being difficult to separate on the thermoanalytical curves.

$BIPE_{0.5ACN}$ has a melting point at 137.6 ± 0.3 °C. The mass loss step in the range 120–150 °C is difficult to observe, given that the amount of solvent bound inside the structure (0.5 mol ACN) is very small. The decomposition process according to the HF curve takes place at slightly higher temperatures than in other solvates, which indicates higher stability of the sample in the presence of this solvent. The mass loss, in this case, is about 67% of the sample mass in the temperature range 339–440 °C.

In the case of $BIPE_{0.35DMSO}$, the thermoanalytical curves obtained at 10 °C min$^{-1}$ in the thermal range 30–500 °C highlight two processes of decomposition: the first in the interval 111.6–143.1 °C with a mass loss of 2.29% of the sample mass, which can be accounted by the loss of the DMSO solvent bound by weak hydrogen bonds within the basic structure of compound BIPE. The HF curve shows the endothermic process of melting the sample with a maximum at 134.7 ± 0.2 °C. The TG curve shows the presence of a decomposition process with a loss of 67% of the sample mass in the range 338.03–437.9 °C. The decomposition process is similar to that observed in the guest-free BIPE, except that the decomposition occurs at higher temperatures by about 20 °C.

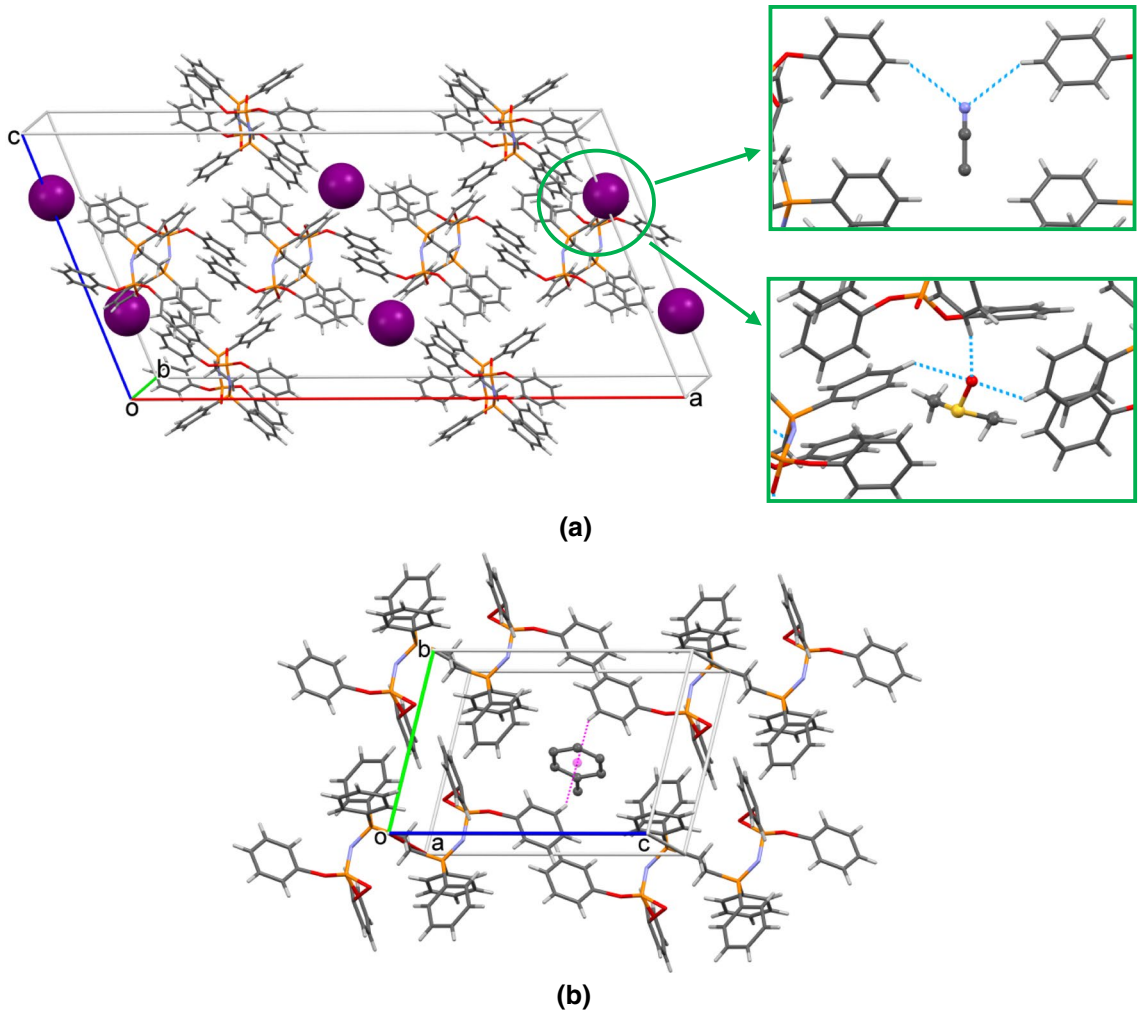


**Fig. 1** Crystal packing in BIPE, $BIPE_{0.5ACN}$ and $BIPE_{0.35DMSO}$. The violet balls show the positions voids (empty or occupied by solvent molecules) in the structure and manner of solvent molecules interaction with surrounding BIPE molecules (**a**). Crystal packing in $BIPE_{TOLUENE}$ structure illustrates the inclusion of toluene (**b**)

**Table 2** Selected geometrical and crystal packing parameters in discussed compounds

| Compound | SG | Unit cell volume/Å$^3$ | Solvent accessible voids (SAVs)/Å$^3$% | Reference |
|---|---|---|---|---|
| BIPE | *C*2/*c* | 8970.3(12) | 322.4 (3.6) | Present work |
| $BIPE_{0.5ACN}$ | *C*2/*c* | 9074.4(9) | 394.9 (4.4)[a] | Present work |
| $BIPE_{0.35DMSO}$ | *C*2/*c* | 9115.5(5) | 432.3 (4.7)[a] | Present work |
| $BIPE_{TOLUENE}$ | $P-1$ | 1265.57 | 229.8 (18.2)[a] | [16] |

[a]SAVs calculated upon the removal of the solvent molecules

The thermal analysis carried out in the case of $BIPE_{TOLUENE}$ shows similarities to $BIPE_{0.35DMSO}$, the decomposition being done by two stages of loss of mass: the first in the range 121.1–147.97 °C with a mass loss of 2% of the sample mass, and the second proceeding in the range 326.1–428.6 °C with a mass loss of 67% of the sample mass similar to the previous ones, which shows that the final stage takes place with the same decomposition process. The melting point of the sample is 136.7 ± 0.3 °C. In the case of $BIPE_{0.35DMSO}$ and $BIPE_{TOLUENE}$ samples, solvent removal occurs before the samples are melted. This is clearly observed on the HF curves obtained for the two samples. In the case of $BIPE_{0.5ACN}$, solvent removal occurs with the sample melting.

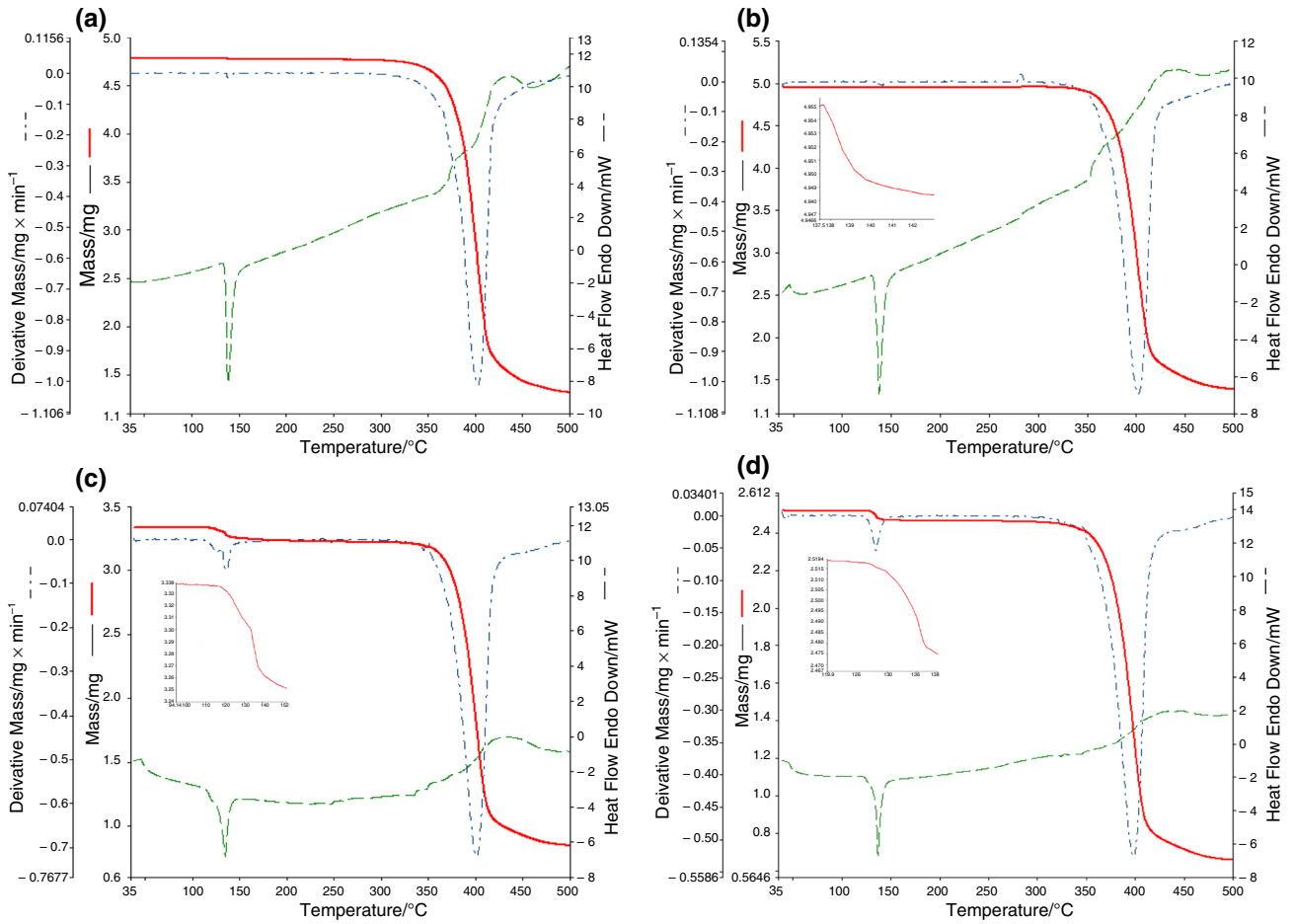


**Fig. 2** Thermoanalytical curves obtained in an air atmosphere with 10 °C $min^{-1}$ in the temperature range 10–500 °C for guest-free BIPE (**a**), $BIPE_{0.5ACN}$ (**b**), $BIPE_{0.35DMSO}$ (**c**) and $BIPE_{TOLUENE}$ (**d**) compounds. *Inset* Zoomed part of the mass loss related to the evaporation of solvents

From the thermogravimetric study performed for the four compounds, it is observed that the solvent is removed differently from the BIPE structure. Thus, the use of DMSO and ACN solvents results in the decomposition of the corresponding solvents at higher temperatures, while in the case of BIPE-$_{TOLUENE}$ the solvent loss occurs at lower temperatures. This can be explained by the size of the solvent molecule.

As the main decomposition process that occurs in all compounds is similar in mass loss (approximately 67%), the kinetic study will aim to analyze the first decomposition step to highlight the influence of the solvent on the thermal behavior of the studied samples. It can be observed that in all cases the residues obtained from the heat treatment carried out in the air atmosphere up to 500 °C represent 25–27% of the mass of the initial samples.

## Kinetic analysis

In the literature, several methods are presented that lead to obtaining kinetic parameters for the solid phase reactions that occur during the decomposition processes.

It is considered that, for an elementary reaction, the expression of the reaction speed can be illustrated by the relation (1) and (2):

$$d\alpha/dt = k(T) \times f(\alpha) \tag{1}$$

where $t$ is the reaction time, temperature $T$ and $\alpha$-conversion degree.

$$(\beta \times d\alpha/dT)_a = k(T) \times f(\alpha) \tag{2}$$

where $\beta$ is the heating rate, $(d\alpha/dT)$ is the direct available DTG data, and $f(\alpha)$ is the conversion function.

The data were obtained at several heating speeds, namely: $\beta = 5$, 7, 10, 12 and 15 °C min$^{-1}$. For obtained the kinetic data, two integral methods were used: Flynn–Wall–Ozawa (FWO) (Eq. 3) [24, 25] and Kissinger–Akahira–Sunose [26, 27] (KAS) (Eq. 4), respectively, and the nonparametric kinetic method (NPK) developed by Sempere et al. [28, 29] modified and developed by Vlase et al. [30, 31].

The Ozawa method uses Eq. 3, being developed by integrating the Arrhenius equation and assumes that neither the activation energy nor the kinetic model changes in the whole reaction.

$$\ln \beta = \ln A/[R \cdot g(\alpha)] - 5.331 - 1.052 \cdot E/R \cdot T \quad (3)$$

$$\ln(\beta/T^2) = \ln[A \cdot R/E \cdot \leq g(\alpha)] - E/R \cdot T \quad (4)$$

Kissinger–Akahira–Sunose uses Eq. 4. The previously presented methods are "model-free" nothing being asserted about the conversion dependence of the reaction rate. Therefore, we decided to use an improved method, named modified NPK method. The mathematical explanation of the method is presented in detail in our previous works [32–37].

Equation (1) is the only assumption made in the development of the nonparametric kinetics (NPK) method.

$$f(\alpha) = \alpha^{m}(1-\alpha)^{n} \quad (5)$$

The kinetic parameters obtained with FWO and KAS methods are centralized in Table 3, and results obtained with NPK methods in Table 4.

Analyzing the results of the kinetic study performed by the FWO and KAS methods, a good correlation between the $\overline{E}$ data of $BIPE_{0.5ACN}$ and $BIPE_{0.35DMSO}$ compounds is observed. The average activation energies are much higher in the case of $BIPE_{0.5ACN}$, which suggests that the bonds formed between the basic structure BIPE and the ACN solvent are much stronger, given that the solvent molecule is smaller and achieves a better organized structure in comparison with $BIPE_{0.35DMSO}$ and $BIPE_{TOLUENE}$.

The results of the NPK analysis are presented in Table 4, which respect the conversion function proposed by Sestak and Berggren [38], as shown in Eq. 5. Regarding the results of the kinetic study carried out by the NPK method, a complex decomposition of $BIPE_{0.5ACN}$ composed by the main process with a mass over 90% ($\lambda = 91.4\%$) and a secondary process is observed here compared to the other compounds. Both processes have deconversion function dependent on chemical ($n \neq 0$) transformations. In the case of $BIPE_{0.35DMSO}$ and $BIPE_{TOLUENE}$, the kinetic study performed by the NPK method revealed three overlapping processes. All main processes have deconversion function dependent on both physical ($m \neq 0$) and chemical ($n \neq 0$) transformations. It is a decomposition followed by melting as seen from the kinetic study performed by the NPK method (chemical and physical process).

**Table 3** Mean activation energy ($\overline{E}$/kJ mol$^{-1}$) determined by the two different kinetic analysis methods

| $\overline{E}_a$/kJ mol$^{-1}$ | Compound | | |
|---|---|---|---|
| | $BIPE_{0.5ACN}$ | $BIPE_{0.35DMSO}$ | $BIPE_{TOLUENE}$ |
| $\overline{E}_a$ (FWO)/kJ mol$^{-1}$ | 424 ± 69 | 212 ± 38 | 291 ± 39 |
| $\overline{E}_a$ (KAS)/kJ mol$^{-1}$ | 440 ± 73 | 216 ± 40 | 365 ± 45 |

## Conclusions

The study provides the synthesis, crystallographic and thermal characterization of guest-free BIPE and its solvates $BIPE_{0.5ACN}$, $BIPE_{0.35DMSO}$ and $BIPE_{TOLUENE}$. All new compounds are isostructural (monoclinic $C2/c$ space group) with similar packing arrangements. The solvent molecules are incorporated in the crystal lattice of the host molecule by weak non-covalent interactions and influence the stability of the structure. The results of the thermogravimetric analyses helped us to assess the thermal stability of the BIPE compounds which reveals high values up to 315 °C for guest-free BIPE and the decrease in the thermal stability to 130–140 °C in the case of solvates. The mass losses were in agreement

**Table 4** Kinetic parameters obtained from NPK

| Compound | Process | $\lambda$/% | $A$/s$^{-1}$ | $E_a$/kJ mol$^{-1}$ | $n$ | $m$ | Corr. coef | Conversion functions | $\overline{E}_a$/kJ mol$^{-1}$ |
|---|---|---|---|---|---|---|---|---|---|
| $BIPE_{0.5ACN}$ | Main | 91.4 | $2.1 \times 10^{54} \pm 1.7 \times 10^{12}$ | 430 ± 21 | 2/5 | 0 | 0.988 | $(1-x)2/5$ | 445 ± 24 |
| | Secondary | 8.2 | $5.2 \times 10^{79} \pm 3.0 \times 10^{20}$ | 630 ± 3 | 5/4 | 0 | 0.999 | $(1-x)5/4$ | |
| $BIPE_{0.35DMSO}$ | Main | 54.3 | $3.5 \times 10^{27} \pm 3.4 \times 10^{12}$ | 211 ± 13 | 1 | 1 | 0.987 | $(1-x) \times x$ | 216 ± 29 |
| | Secondary 1 | 31.1 | $6.8 \times 10^{31} \pm 1.6 \times 10^{16}$ | 244 ± 10 | 0 | 3/2 | 0.999 | $x^{3/2}$ | |
| | Secondary 2 | 14.6 | $6.8 \times 10^{31} \pm 5.3 \times 10^{24}$ | 175 ± 7 | 1 | 1 | 0.997 | $(1-x) \times x$ | |
| $BIPE_{TOLUENE}$ | Main | 90.8 | $1.5 \times 10^{39} \pm 5.8 \times 10^{21}$ | 302 ± 36 | 1 | 1 | 0.994 | $(1-x) \times x$ | 293 ± 44 |
| | Secondary 1 | 5.7 | $9.9 \times 10^{2} \pm 9.6 \times 10^{1}$ | 15 ± 5 | 1 | 1 | 0.992 | $(1-x) \times x$ | |
| | Secondary 2 | 3.5 | $9.9 \times 10^{2} \pm 5.8 \times 10^{1}$ | 507 ± 2 | 0 | 3/2 | 0.999 | $x3/2$ | |

with the stoichiometric solvent amount incorporated in solvates. We can conclude that nature of the solvent dictates the stability of solvates as follows: toluene < ACN ~ DMSO. In addition, the kinetic study provides a more complete picture of the degradation process of BIPE solvates. The kinetic parameters were determined by using three different methods FWO, KAS and NPK. The first two methods provide average activation energies much higher for $BIPE_{0.5ACN}$ in comparison with the other studied solvates, correlating with higher thermal stability. NPK method shows a better understanding of the multistep degradation processes, revealing a deconversion function dependent on both physical and chemical transformations.

**Acknowledgements** This work was partially supported by Program 2, Project 2.1 of the "Coriolan Drăgulescu" Institute of Chemistry and by Project ANCD 20.80009.5007.15 of the Institute of Applied Physics.

## References


1. Healy AM, Worku ZA, Kumar D, Madi AM. Pharmaceutical solvates, hydrates and amorphous forms: a special emphasis on cocrystals. Adv Drug Deliv Rev. 2017;117:25–46.
2. Chadha R, Kuhad A, Arora P, Kishor S. Characterisation and evaluation of pharmaceutical solvates of Atorvastatin calcium by thermoanalytical and spectroscopic studies. Chem Cent J. 2012;6:114–29.
3. Griesser UJ. The importance of solvates. In: Weinheim HR, editor. Polymorphism in the Pharmaceutical Industry. Hoboken: Wiley; 2006. p. 211–233.
4. Görbitz CH, Torgersen E. Symmetry, pseudosymmetry and packing disorder in the alcohol solvates of L-leucyl-L-valine. Acta Cryst B. 1999;B55:104–13.
5. Tieger E, Kiss V, Pokol G, Finta Z, Rohlicek J, Skorepova E, Dusek M. Rationalization of the formation and stability of bosutinib solvated forms. Cryst Eng Commun. 2016;18:9260–74.
6. Vippagunta SR, Brittain HG, Grant DJW. Crystalline solids. Adv Drug Deliv Rev. 2001;48:3–26.
7. Barbour LJ. Organic cage crystals: supramolecular joinery. Nat Chem. 2015;7:97–9.
8. Hosokawa T, Datta S, Sheth AR, Brooks NR, Young VG, Grant DJW. Isostructurality among five solvates of phenylbutazone. Cryst Growth Des. 2004;4:1195–201.
9. Sarma JARP, Desiraju GR. Polymorphism and pseudopolymorphism in organic crystals: A Cambridge Structural Database study. In: Seddon KR, Zaworotko M, editors. Crystal engineering: design and application of functional solids. Dordrecht: Kluwer Academic Publishers; 1999. p. 325–356.
10. Caira MR, Bettinetti G, Sorrenti M. Structural relationships, thermal properties, and physicochemical characterization of anhydrous and solvated crystalline forms of tetroxoprim. J Pharm Sci. 2002;91:467–81.
11. Görbitz CH, Hersleth HP. On the inclusion of solvent molecules in the crystal structures of organic compounds. Acta Cryst B. 2000;B56:526–34.
12. Desiraju GR, Sharma CVK. Perspectives in supramolecular chemistry: the crystal as supramolecular entity. In: Desiraju GR, editor. Chichester: Wiley; 1996. p. 31–61.
13. Gololobov YG, Kasukhin LF. Recent advances in the Staudinger reaction. Tetrahedron. 1992;48:1353–406.
14. Molina P, Vilaplana MJ. Iminophosphoranes: useful building blocks for the preparation of nitrogen-containing heterocycles. Synthesis. 1994;194:1197–218.
15. Stolzenberg H, Weinberger B, Fehlhammer WP, Puhlhofer FG, Weiss R. Free and metal-coordinated (N-Isocyanimino)triphenylphosphorane: X-ray structures and selected reactions. Eur J Inorg Chem. 2005;21:4263–71.
16. Staudinger H, Mayer J. Über neue organische Phosphorverbindungen III Phosphinmethylenderivate und Phosphinimine. Helv Chim Acta. 1919;2:635–46.
17. Weller F, Kang HC, Massa W, Rübenstahl T, Kunkel F, Dehnicke K. Crystal structures of the Silylated Phosphanimines $Me_3SiNPPh_3$ und $Me_3SiNPPh_2–C_2H_4–PPh_2NSiMe_3$. Z Naturforsch B J Chem Sci. 2014;50(7):1050–4.
18. Marsh RE. The space groups of point group $C_3$: some corrections, some comments. Acta Cryst B. 2002;58:893–9.
19. Micle A, Miklašova N, Varga RA, Pascariu A, Plesu N, Petric M, Ilia G. A versatile synthesis of a new bisiminophosphorane. Tetrahedron Lett. 2009;50:5622–4.
20. Petric MF, Crisan ME, Chimakov YM, Varga RA, Micle A, Neda I, Ilia G. Structural and ab initio studies on the polymorphism of iminophosphorane $(CH_3C_6H_4)_3P=NP[(=O)(OPh)_2]$. J Mol Struct. 2015;1083:389–97.
21. Sheldrick GM. Crystal structure refinement with SHELXL. Acta Cryst C. 2015;C71:3–8.
22. Macrae CF, Edgington PR, McCabe P, Pidcock E, Shields GP, Taylor R, Towler M, Van de Streek J. Mercury: visualization and analysis of crystal structures. J Appl Cryst. 2006;39:453–7.
23. Spek AL. Structure validation in chemical crystallography. Acta Cryst D. 2009;D65:148–55.
24. Ozawa T. A new method of analyzing thermogravimetric data. Bull Chem Soc Jpn. 1965;38:1881–6.
25. Flynn JH, Wall LA. A quick, direct method for the determination of activation energy from thermogravimetric data. Polym Lett. 1966;4:323–8.
26. Kissinger HE. Reaction kinetics in differential thermal analysis. Anal Chem. 1957;29(11):1702–6.
27. Akahira T, Sunose T. Joint convention of four electrical institutes. Research report Chiba institute of technology. Sci Technol. 1971;16:22–31.
28. Serra R, Nomen R, Sempere J. The non-parametric kinetics. A new method for the kinetic study of thermoanalytical data. J Therm Anal Calorim. 1998;52:933–43.
29. Serra R, Sempere J, Nomen R. A new method for the kinetic study of thermoanalytical data: the non-parametric kinetics method. Thermochim Acta. 1998;316:37–45.
30. Vlase T, Vlase G, Doca N, Bolcu C. Processing of non-isothermal TG data. Comparative kinetic analysis with NPK method. J Therm Anal Calorim. 2005;80:59–64.
31. Vlase T, Vlase G, Birta N, Doca N. Comparative results of kinetic data obtained with different methods for complex decomposition step. J Therm Anal Calorim. 2007;88:631–5.
32. Vlase G, Bolcu C, Modra D, Budiul MM, Ledeți I, Albu P, Vlase T. Thermal behavior of phthalic anhydride-based polyesters. J Therm Anal Calorim. 2016;126:287–92.
33. Ceban I, Blajovan R, Vlase G, Albu P, Koppandi O, Vlase T. Thermoanalytical measurements conducted on repaglinide to estimate the kinetic triplet followed by compatibility studies between the antidiabetic agent and various excipients. J Therm Anal Calorim. 2016;126:195–204.
34. Patrutescu C, Vlase G, Turcus V, Ardelean D, Vlase T, Albu P. TG/DTG/DTA data used for determining the kinetic parameters of the thermal degradation process of an immunosuppressive agent: mycophenolate mofetil. J Therm Anal Calorim. 2015;121(3):983–8.

35. Vlase T, Vlase G, Doca N. Kinetics of thermal decomposition of alkaline phosphates. J Therm Anal Calorim. 2005;80(1):207–10.
36. Albu P, Doca SC, Anghel A, Vlase G, Vlase T. Thermal behavior of sodium alendronate. J Therm Anal Calorim. 2017;127(1):571–6.
37. Paul A, Budiul M, Mateescu M, Chiriac V, Vlase G, Vlase T. Studies regarding the induced thermal degradation, kinetic analysis and possible interactions with various excipients of an osseointegration agent-zoledronic acid. J Therm Anal Calorim. 2017;130(1):403–11.
38. Sestak J, Berggren G. Study of the kinetics of the mechanism of solid-state reactions at increasing temperatures. Thermochim Acta. 1971;3:1–12.